An experimentalist's highlights

Maria Novella Kienzle-Focacci [a]

[a]University of Geneva, DPNC, 24 quai E. Ansermet,
1211 Genève 4, Switzerland

A concise summary of recent experimental data presented at this conference illustrates the progress in our understanding of the photon interactions. The perturbative QCD domain of high Q^2 two-photon events and high p_t jet production in both $\gamma\gamma$ and eγ interactions is well described by NLO calculations and parton density functions. Measurements of diffractive processes and resonance formation provide a detailed information on the difficult field of long range strong interaction forces.

1. INTRODUCTION

In the last years hadron production has been studied in a large variety of channels in photoproduction and deep inelastic scattering at HERA and in two-photon collisions at LEP (LEP1, $\sqrt{s} \simeq 91$ GeV, and LEP2, $\sqrt{s}> 160$ GeV). I will focus on the main achievements of the analyses, leaving to the individual talks the detailed discussion of the data.

I will avoid the mathematical definition of the variables used, for which I refer to the introductory talks [1] - [4] and to the individual presentations. I only need to clarify some terminology. The label "direct" or "resolved" process describes the photon behaviour in the interaction: "direct", if the photon interacts as a pointlike particle, "resolved" if a partonic constituent of the photon participates in the interaction. A variable x_γ can be defined experimentally, it measures the momentum of the interacting particle, relative to the photon momentum : $x_\gamma= 1$ for a direct process, $x_\gamma<1$ for a resolved process. In two-photon physics both photons interact as pointlike in the "direct process" $\gamma\gamma\to q\bar{q}$, a QED interaction at the first order; at HERA the "direct process" is the photon-gluon fusion γg $\to q\bar{q}$, where the gluon is a parton of the proton. For two-photon physics this is already a "single-resolved" process and the "resolved" process of HERA gg $\to q\bar{q}$ is a "double-resolved" process.

2. PHOTON STRUCTURE

2.1. F_2^γ at LEP

Final LEP1 results on the single-tag process $e^+e^-\to e^+e^-$hadrons are now available in published [5] or preliminary form [6],[7],[8] . The limited acceptance of the hadrons in the detectors is the main concern of this analysis.The problem was illustrated by Armin Böhrer (Fig.1) : x_{vis} is a faithful measurement of x (x $= Q^2/(Q^2+ W_{\gamma\gamma}{}^2)$)

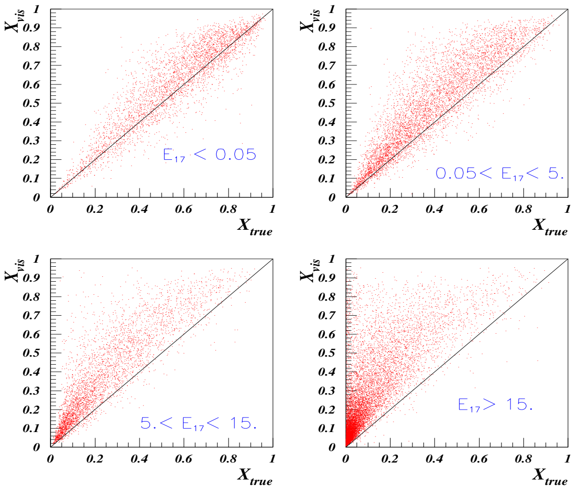

Figure 1. *Correspondence between the measured x ($x_{\rm vis}$) and the true value ($x_{\rm true}$) for different energies emitted in a forward cone of* 17° *[6].*

if the energy emitted in a cone of 17° around the beam is small,while the measurement becomes more and more unreliable as the energy emitted in the forward cone increases.

Several methods have been used by the experiments to reduce this effect :

- ALEPH and OPAL perform a two-dimensional unfolding using the energy in the forward cone as the second variable.

- L3 uses the constraint of the transverse momentum and, for high Q^2 events, performs a kinematical fit in which the missing energy is included in the resolution. This method requires a very careful study of the detector and it is not clear if the successful analysis presented by F. Erne [5] can be applied also in Q^2 and x regions not dominated by the direct process.

These methods improve the resolution of x and reduce the bin-to-bin correlation but they don't avoid the problem of the Monte Carlo unfolding. The LEP working group [9] has analysed this effect by comparing the most sensitive hadronic distributions of the four LEP experiments. Although the four detectors have a different acceptance, the experimental data agree rather well, differences being of the order of the statistical errors, while by correcting the data with different models (HERWIG [10] and PHOJET [11] have been investigated) the differences can be many standard deviations higher than the experimental differences. The dependence of the results on the Monte Carlo used is therefore always present, even if the generators have much improved since the first LEP analyses [13]. By inspection of the data one sees that this problem is serious only at low x and low Q^2, precisely in the region where the partonic content of the photon plays a dominant role. We can think of improving the models by a systematic comparison of the general purpose Monte Carlo with the data, as R. Taylor and J.Butterworth showed [14]. I would recommend that, until this optimization is done, the results should not be presented as an average of unfolding using different Monte Carlo's, since in this way it is difficult to recover the "truly experimental" value. A compilation of the most recent LEP data on F_2^γ is shown in Fig.2 as a function of Q^2 for different x intervals.

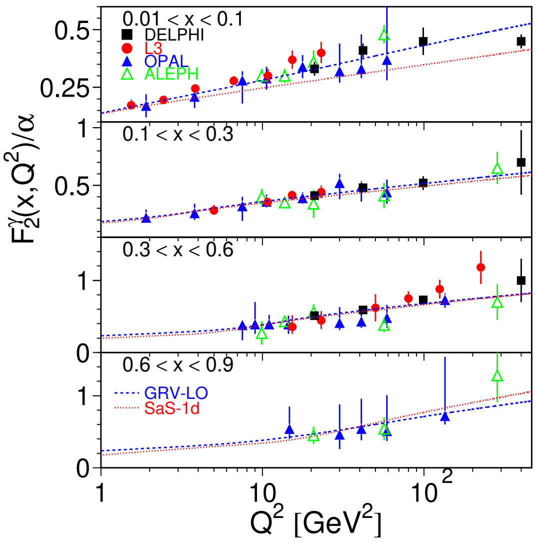

Figure 2. *The Q^2 evolution of the hadronic structure function F_2^γ as measured at LEP.*

Superimposed on the data are predictions of the parton density functions (pdf) SaS-1d [15] and GRV [16]; GRV pdf gives, at present, the best description of the data. ALEPH [6] presented a very complete comparison of its data with the existing pdf. The authors conclude that the models with large gluon content do not fit $F_2^\gamma(x,Q^2)$.

In comparing the data another point must be clarified : how the experiments take into account the non-zero virtuality of the target photon. As proven by the leptonic structure function analysis, this effect is non negligible [1].

In conclusion LEP1 data seem ready for a combined fit in order to get a new set of partonic density functions. What next? LEP2 data will improve the statistical accuracy of the high Q^2 range and we could envisage an evaluation of $\Lambda_{\rm QCD}$ from the values of F_2^γ measured at high

x. The study of azimuthal correlations in $e^+e^- \to e^+e^-\mu^+\mu^-$ data [17] shows that the longitudinal structure function is accessible by measuring the interference term F_A^γ (Fig.3). It would be interesting to see this study performed with two-jet events; the jets should also provide a wider angular coverage than the muons.

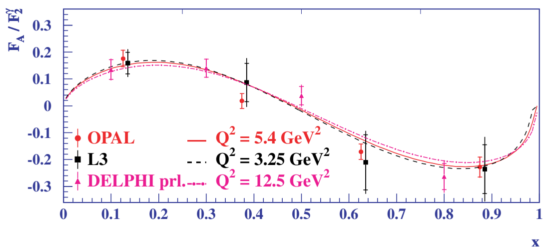

Figure 3. *The structure function F_A^γ/F_2^γ, obtained by azimuthal correlations in the $e^+e^- \to e^+e^-\mu^+\mu^-$ channel [1].*

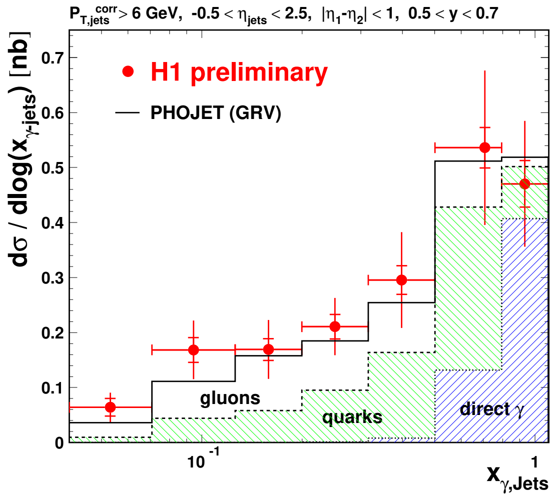

Figure 4. *The x_γ distribution which allow to separate different processes in the jet analysis at HERA [19].*

2.2. Photon structure from jets and inclusive single particle production at HERA

From e^+e^- single-tag two-photon events the photon structure function is measured within a deep inelastic scattering formalism, similar to the one used for the proton structure function. The cross-sections of high p_t jets and single particle production measured at HERA and at LEP also probe the photon structure, but the measurement is more indirect since it depends on theoretical calculations (at present NLO QCD calculations are available), on the definition of a jet and on the fragmentation function if a single particle is studied. From the measurement of differential cross-sections one can extract effective parton densities of quarks and gluons in the photon. At HERA the photon structure has been studied also as function of the photon virtuality Q^2. The pointlike interaction of the photon (direct) and the resolved contribution are separated by using the x_γ variable (Fig.4).

This distribution is well understood if the radius of the jet is restricted, or if the transverse energy of the jet is high (E_T>14 GeV), or if Q^2> 0.1 GeV^2. Outside these limits the soft underlying events, due to soft peripheral collisions or to semi-hard multi-particle interactions, generate an excess of events at low x_γ, hardly reproduced by Monte Carlo models [20].

An impressive number of channels have been studied: inclusive jet [18], dijet [19] and multi-jet [20] events , single photon [21], J/Ψ [22] and D*[23], [24] production. This is what we learned:

- The resolved photon contribution decreases with increasing Q^2 [25]. The decrease, much slower than the one observed for vector meson production, is expected by perturbative QCD : in the region $\Lambda^2_{QCD} < Q^2 < E_T{}^2$ the probability of finding a quark in the virtual photon should decrease as $\ln(E_T{}^2/Q^2)$ (Fig.5).

- NLO calculations, with the GRV pdf, reproduce in general the dijet cross section in shape and magnitude, except when both jets are forward relative to the proton direction [20].

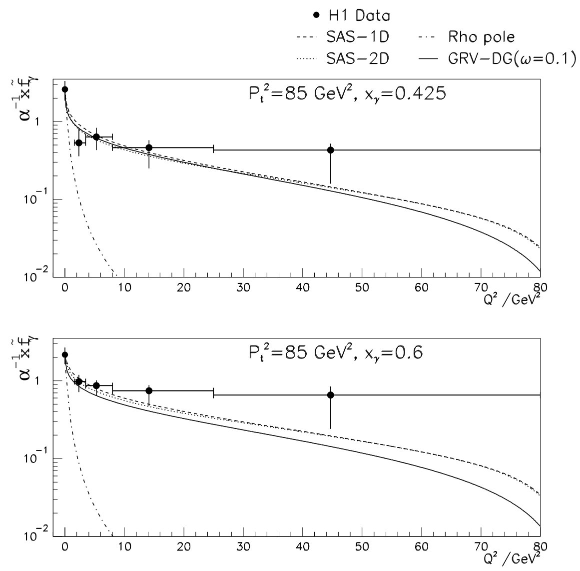

Figure 5. *The dependence of the effective parton density in the photon on the photon virtuality Q^2 [25].*

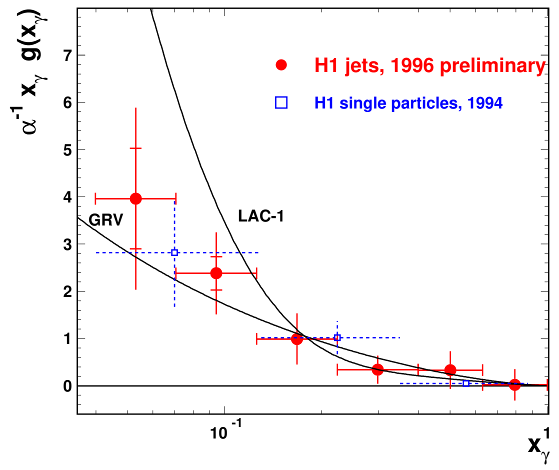

Figure 6. *The gluon distribution in the photon, extracted by the jet and single particle differential cross section [19].*

- From the differential cross section $d^4\sigma/dydx_\gamma dx_p d\cos\theta^*$ of jets and single particle production [19], H1 extract an effective gluon distribution (Fig.6) in the photon, somewhat higher at low x_γ than expected by the GRV pdf. One notice also a systematic discrepancy of 5-25% between the results obtained by correcting the data with PYTHIA or with PHOJET, in Fig.6 the average value is plotted.

- For three-jet events, ZEUS analyses the angular distribution of the third, least energetic jet (Fig.7). This is clearly not a phase space distribution (dotted line). It is explained by $O(\alpha\alpha_s)$ calculations. The data also require colour coherence, as demonstrated by a Monte Carlo comparison [20].

- From the analysis of four-jet events, H1 identifies the γ-remnant jet as the jet closest to the γ^* direction. This analysis show that the average p_t in the remnant jet has

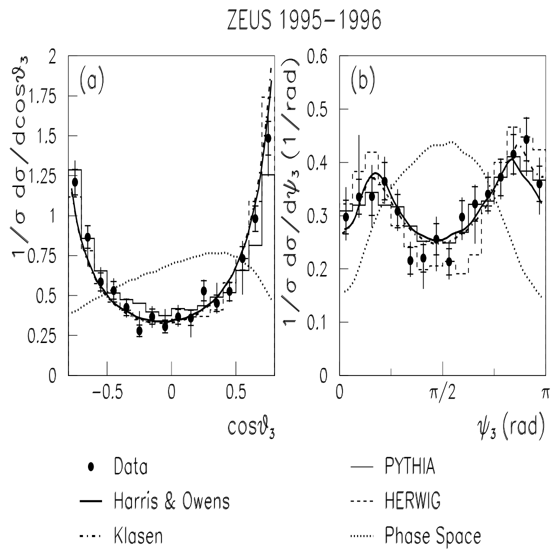

Figure 7. *The angular distribution of the least energetic jet in ZEUS three-jet analysis [20].*

a weak dependence on the photon virtuality Q^2, but is correlated to the scale of the hard process [26].

- Prompt photons have been identified [21] isolated or together with a jet. Here the direct process $\gamma q \to \gamma q$ is dominant. The NLO QCD predictions agree with the measured cross sections if the GRV pdf is used (Fig.8)

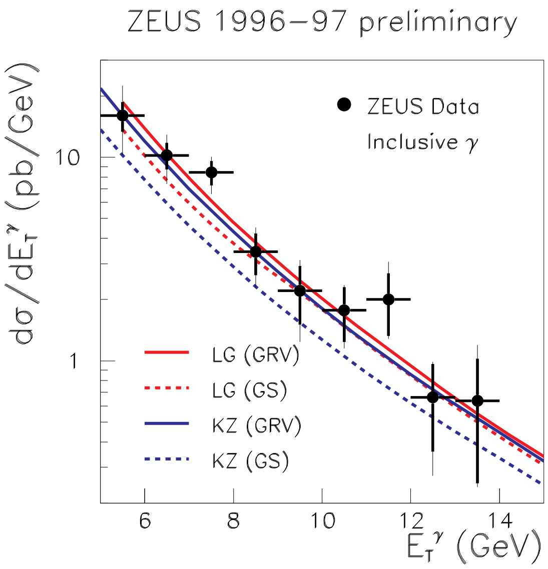

Figure 8. *Direct photon production compared to NLO calculations [21].*

2.3. Unexpected : b at HERA

Both H1 [23] and ZEUS [24] showed evidence of significant b production. The b-quark is tagged by a muon (H1) or an electron (ZEUS) which have large p_t relative to the jet axis. This signal came as a surprise since the observed cross-sections are higher than expected. The cross section measured by H1 inside the detector acceptance is : $\sigma_{b\bar{b}} = 0.93 \pm 0.08^{+0.21}_{-0.12}$ nb for an expected value of 0.19 nb.

2.4. Jets and single particle production at LEP

At LEP only OPAL [27] measured high p_t jets, charged hadron and K^0_S production. For dijet events the x_γ distribution separates the direct from resolved processes. As already observed at HERA [28], the angular distribution in the dijet center-of-mass shows a clear difference between the direct, $\gamma\gamma \to q\bar{q}$ process, where a quark is exchanged in the t-channel and the resolved processes, dominated by gluon exchange (Fig.9).

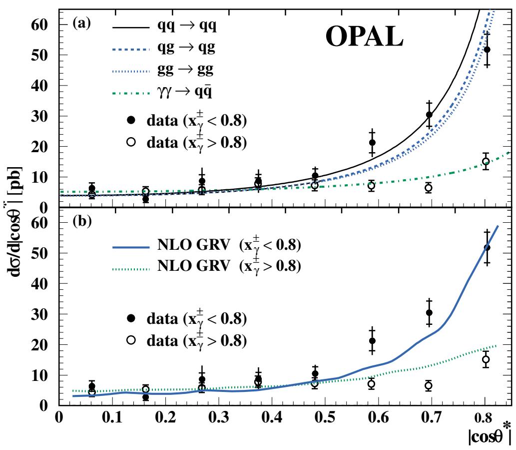

Figure 9. *The angular distribution in the dijet center-of-mass system for "direct" and "resolved" events [27].*

The jet and inclusive single-particle differential cross sections agree well with NLO calculations, using GRV pdf (Fig.10 top). All processes are necessary : the direct contribution is dominant at high p_t, the double resolved process (gg → gg) is necessary at low p_t values. It is also interesting to compare the p_t distribution of charged hadron produced by different interactions ($\gamma\gamma$, γp and πp) (Fig.10 bottom). While the p_t spectrum of hadrons in photoproduction is similar to the one observed in pure hadronic interactions, the spectrum measured in two-photon interactions is harder due to the direct γq coupling. OPAL notice also that PHOJET and PYTHIA both underestimate the K^0_S production by $\simeq 30$ %.

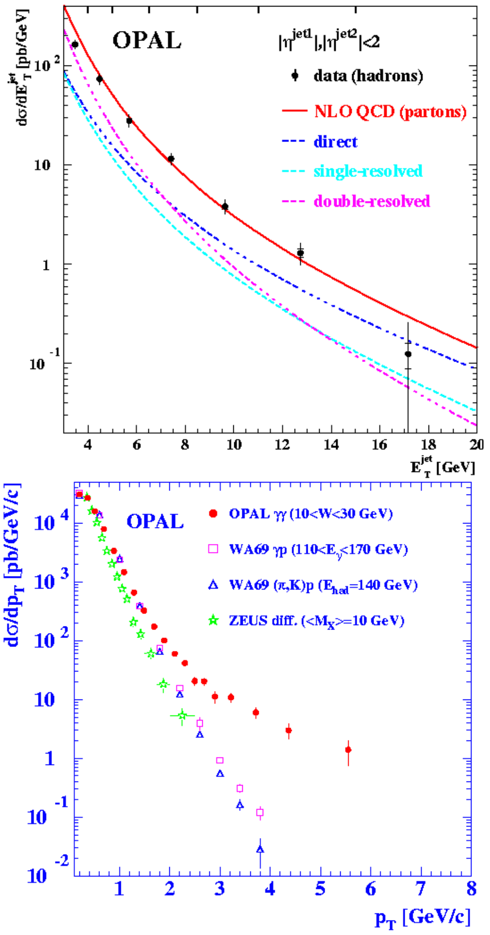

Figure 10. *Differential cross-section as a function of p_t for jets (top) and for charged hadron production (bottom) [27].*

3. TWO-PHOTON CROSS-SECTIONS

3.1. Total $\gamma\gamma$ cross-section

During the LEP2 workshop [29] it was stated that it would be very difficult to measure the two-photon total cross-section. This conclusion was based on the data obtained at low energy colliders, where the separation between two-photon and annihilation events is problematic. At LEP2 the two-photon processes are the dominant source of hadrons and they are easily separated from the annihilation channels. The analysis can be performed with a low background in a large $W_{\gamma\gamma}$ mass range. We must also remember that, in all experiments at LEP, there is now a strong pressure from the new particle searches for a better understanding of the two-photon hadronic processes, because they can obscure completely the signal of new phenomena in some kinematical region. Two-photon total cross-sections have been

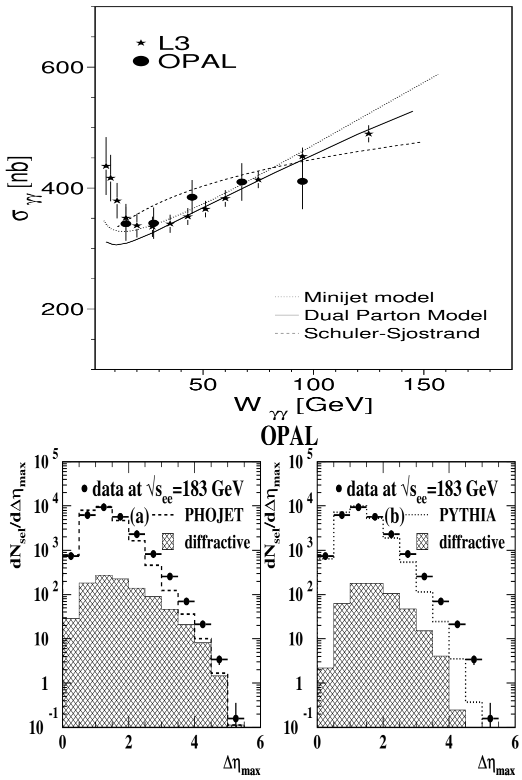

Figure 11. *(top) Two-photon total cross-section compared to models which take into account the direct γq coupling [33],[11],[34]. Both samples of data[30],[31] are unfolded with PHOJET. (bottom) The diffractive component is shown for the rapidity distribution of hadrons; it has a different shape in the PYTHIA and PHOJET generators.*

measured by L3 [30] and OPAL [31] in the mass range 5 GeV $< W_{\gamma\gamma} <$ 145 GeV. The two models employed to correct the data, PYTHIA and PHOJET, give a difference of $\sim$20% in the absolute scale of $\sigma_{\gamma\gamma}$. The measurements of the two experiments agree if the same Monte Carlo is used (Fig.11 top). The unfolding procedure introduces a strong bin-to-bin correlation which must be taken into account when fitting the data. The cross-section shows the typical behaviour of hadron-hadron total cross-sections : a fast decrease for $W_{\gamma\gamma} <$ 20 GeV, due to reggeon exchange, and a slow increase at higher energies, described by a "soft" Pomeron. The rise of $\sigma_{\gamma\gamma}$ is faster than the one observed in hadron-hadron or γp cross-sections; a simple factorisation ansatz $\sigma_{\gamma\gamma} = \sigma^2_{\gamma \mathrm{p}}/\sigma_{\mathrm{pp}}$ is excluded. The $W_{\gamma\gamma}$ dependence is rather well described by most of the models which take into account the direct γq coupling [32], [33].

The different results obtained by correcting the data with different generators may be related to the description of the diffractive component (Fig.11 bottom) for which the detectors acceptance is small. L3 has investigated the diffractive contribution by studying exclusive and inclusive ρ^0 production [30]. In the limited kinematical range accessible to the experiment both generators fail to reproduce the data : PHOJET predicts too few ρ^0 events while the almost constant production in $W_{\gamma\gamma}$, predicted by PYTHIA, is not observed in the measured range 3 $< W_{\gamma\gamma} <$ 8 GeV.

3.2. Double tag measurements

When both scattered electrons are detected, the $W_{\gamma\gamma}$ variable can be measured from the four-momenta of the two scattered electrons, thus strongly reducing the model dependence of the cross-section measurement. OPAL [35] and L3 [36] presented their results. The data agree with Monte Carlo predictions (Fig.12), while the BFKL LO calculations [37], which focused our interest on this measurement, predict much too high values (Fig.13). Also recent BFKL calculations [38] which take into account NLO effects fail to reproduce the data [35],[36].

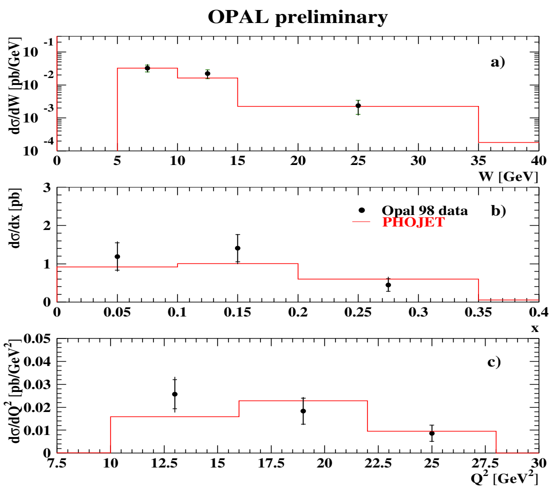

Figure 12. *The differential cross-section of double tag events compared to PHOJET Monte Carlo predictions [35].*

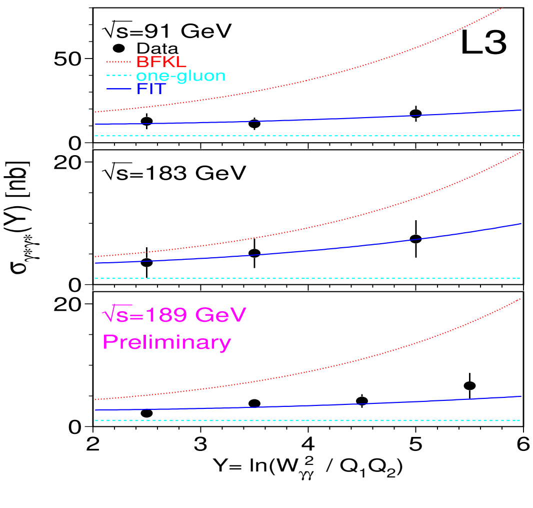

Figure 13. *The two-photon cross-sections obtained with double-tagged events at LEP1 and LEP2. They are compared to LO-BFKL calculations after subtraction of the direct contribution [36].*

3.3. Inclusive c and b production

Inclusive charm production is well suited to study direct and resolved processes due to the high mass of the c-quark, that provides a natural hard scale for pQCD calculations. The resolved contribution is dominated by quark-gluon fusion, $\gamma g \rightarrow c\bar{c}$, thus this measurement can provide a strong constraint for the determination of the gluon content of the photon. These data have been presented by L3 [39], which tags the charm-quark with leptons and with $D^* \rightarrow D^0\pi$, $D^0 \rightarrow K^-\pi^+$, and by OPAL [40] which tags the charm-quark with $D^* \rightarrow D^0\pi$, $D^0 \rightarrow K^-\pi^+$ and $K^-\pi^+\pi^-\pi^+$.

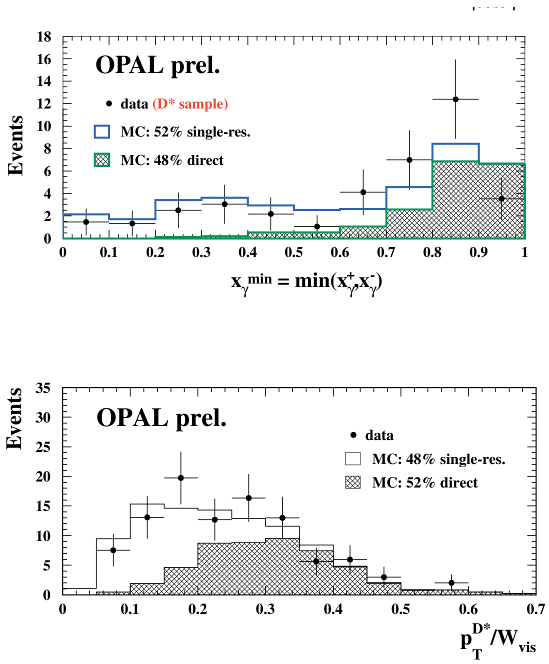

Figure 14. *(top) The x_γ distribution of dijet events containing a D^*. (bottom) The p_t distribution of the D^* normalised to the visible mass of the event [40].*

A good separation of direct and resolved processes is obtained by associating the D^* to a dijet analysis or by inspection of the p_t distribution of the D^* (Fig.14). At LEP2 energies the direct and resolved processes contribute equally to the cross-section. The differential D^* cross section agrees well with NLO calculations. The dependence on the pdf's, on the factorisation and renormalisation scales are small. Differential cross-sections, measured inside the kinematical range of the detector acceptance, are also rather independent on the Monte Carlo models used for efficiency corrections. With a stronger model dependence the data are extrapolated to the total charm production cross-section (Fig.15). In this figure also the b production cross-section is shown, as it has been measured for the first time by L3, by tagging high p_t leptons (electrons and muons), with an analysis similar to the one performed at HERA.

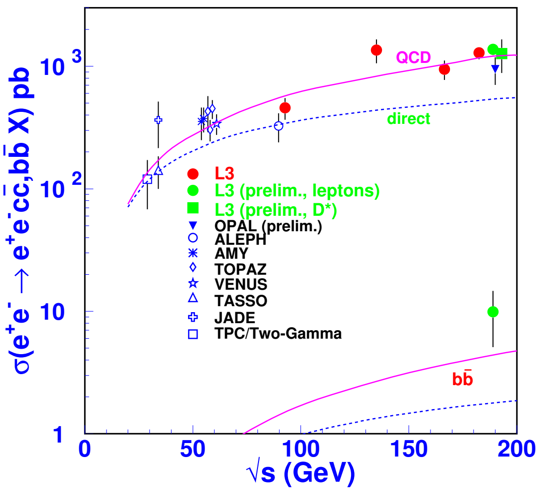

Figure 15. *The cross-section for heavy quarks production as measured at LEP and at previous* e^+e^- *colliders [39].*

4. DIFFRACTION AT HERA

An impressive large amount of studies on diffractive events has been undertaken at HERA. A diffractive process (Fig.16 top) is signed by a leading baryon (p and n can be measured in the very forward detectors [41]) or by a large rapidity gap between two-jets, X and Y, observed in the reaction ep → e′ X Y, or by an excess in the X mass distribution. Traditionally the elastic and diffractive phenomena are described by Regge-pole models where the exchanged fields are Regge trajectories with the quantum numbers of resonances, or the Pomeron trajectory with the vacuum quantum numbers. From the measurement of differential diffractive cross-sections H1 and ZEUS extract an effective "Pomeron" structure function and determine the slope and the intercept of the Pomeron trajectory.

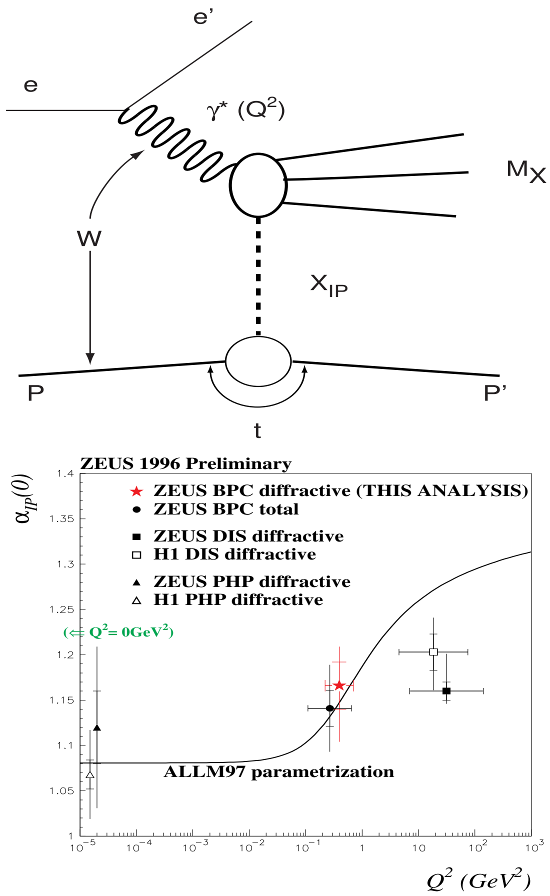

Figure 16. *(top) Definition of the variables in a diffractive process. (bottom) The intercept of the Pomeron trajectory as a function of Q^2 [43].*

About 10% of the events are found to be diffractive, this is maintained also in events where a D* is present [42]. Many features of the events have been studied [43] and the challenge is to understand what is a Pomeron. Clearly it is not just a single Regge pole as proven by the different values of the intercept obtained for different Q^2 (Fig.16 bottom). Is it a $q\bar{q}$ colour singlet or a gluon ladder? A gluon dominated Pomeron seems to describe well HERA data, in contradiction with diffractive measurements at Fermilab which don't support more than ≃ 40 % of a gluon component in the Pomeron.

4.1. Elastic vector meson production

The nature of the Pomeron is extensively investigated in elastic vector meson production ep → e′ V p′ [44]. Information on the production of all vectors is available, from light vectors (ρ, ω, ϕ) to the J/ψ and Υ (Fig.17). Vector production has been measured as a function of hard scales: Q^2, t, M_V (see Fig.16 top). While the Vector

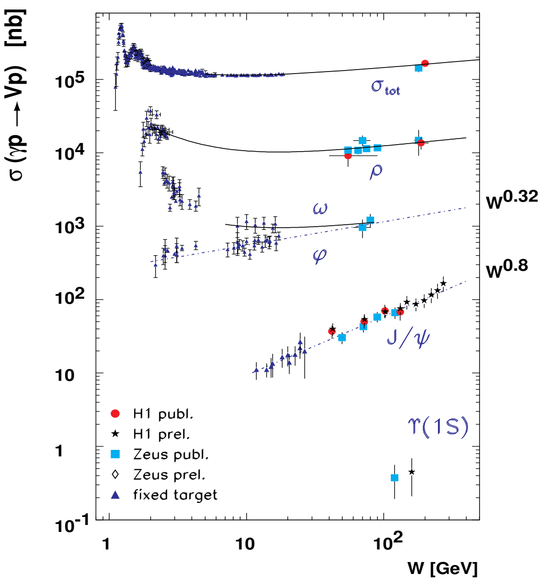

Figure 17. *The photoproduction cross-section and the elastic vector meson production as a function of the γp center-of-mass energy [44].*

Dominance Model and a "soft" Pomeron describe the data in the absence of an hard scale, a more complex behaviour appear when an hard scale is present. Perturbative QCD may explain some of these effects by considering a strong influence of the gluons and of the quark mass in the interaction.

The spin-density matrix of the ρ have been measured. A small violation of the s-channel helicity conservation is observed at high Q^2. The ratio of longitudinal to transverse cross-section rises with Q^2 as expected by QCD (Fig.18). Double flip contributions, increasing with |t|, have been observed by ZEUS.

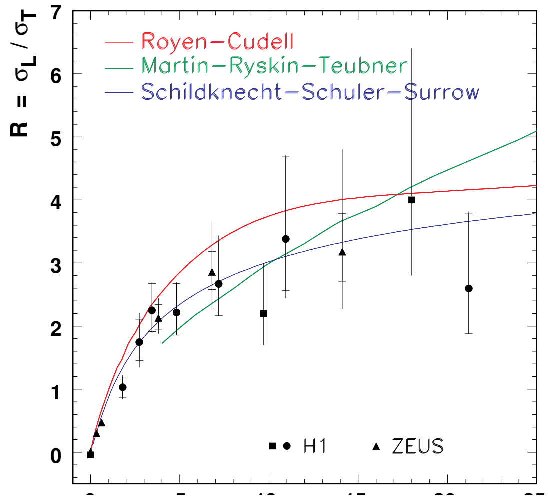

Figure 18. *The ratio of longitudinal to transverse cross-section for elastic ρ electroproduction [44].*

The first polarization measurements at HERMES have been presented [45]. The cross-sections and the decay angle distributions will be measured for all vectors as well as the double-spin asymmetries.

In conclusion a large variety of diffractive phenomena are studied at HERA. This is the domain where the reliable, perturbative QCD calculations no longer apply, leaving the place to the successful phenomenology of Regge theory. The main objective of experimental and theoretical work is to understand the link between the two descriptions.

5. RESONANCE FORMATION AT LEP

Resonance formation in two-photon collisions provide an important test for gluonium candidates [46], since the two-photon width of a gluon rich hadron must be significantly smaller than the one measured for normal $q\bar{q}$ states. L3 [47] gets a limit of 1.5 eV at 95% CL for the ξ (2230) production in the $K^0_S K^0_S$ decay channel, for which CLEO has a limit of 1.3 eV. CLEO presented also a limit of 2.5 eV for the $\pi^+\pi^-$ decay of the ξ (2230) [46].

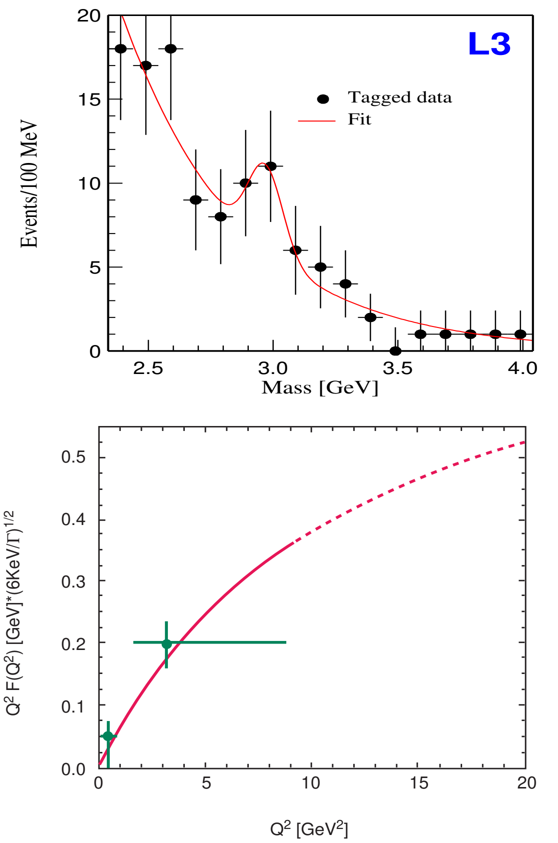

Figure 19. *(top) The η_c signal for single-tag events [50]. (bottom) The measured η_c form-factor compared to QCD calculations [52].*

These measurements give a strong support to the interpretation of this resonance, observed in J/ψ decay [48], as a glueball state; a confirmation of its existence in a gluon rich environment would be welcome. The $\eta(1440)$, observed for the first time in untagged two-photon events by L3 [49], has a value of $\Gamma_{\gamma\gamma}\times$ Br(K $\bar{\rm K}\pi$)= 166 $\pm$ 52 eV, thus excluding a gluonium interpretation of this resonance.

New measurements for charmonium states were presented by L3 [50] and by E835 [51]. L3 measured the η_c form-factor (Fig.19) by tagging a scattered electron in the forward calorimeters. The data strongly favours a form factor with a J/ψ pole and are well in agreement with theoretical calculations [52].

The two-photon width of the η_c, measured in two-photon formation, is well in agreement with the value measured in $p\bar{p} \rightarrow \gamma\gamma$ annihilation. In contrast, for the χ_{c2} a discrepancy of $\sim$ 3 standard deviations subsists. The combined two-photon results [53] is $\Gamma_{\gamma\gamma}(\chi_{c2}) = 1.23 \pm 0.23$ keV and the new $p\bar{p}$ measurement of E835 [51] (Fig.20 bottom), $\Gamma_{\gamma\gamma}$= 0.31 $\pm$ 0.05 $\pm$ 0.04 keV confirms the previous E760 measurement [54]. The $p\bar{p}$ measurement doesn't need any external input, since the total width of the resonance and the $\chi_{c2}$$\rightarrow$$p\bar{p}$ branching ratio is obtained from the $p\bar{p}$ $\rightarrow$J/$\psi\gamma$ spectrum (Fig.20 top). As pointed out by A. Buijs, all two-photon experiments use the $\chi_{c2}$$\rightarrow$J/$\psi\gamma$ decay channel and the very low energy photon ($\simeq$ 300 MeV) lies in a steeply falling spectrum. This can be the cause of a misinterpretation of the background.

No η_c' signal is observed either at LEP, where DELPHI [55] and L3 [50] searched for it, or in $p\bar{p}$ annihilation [51].

6. CONCLUSIONS

The large number of data analyses, performed at HERA and LEP should help us to better understand the complex nature of the photon and of the Pomeron.

More data will be available in the near future, but, in order to improve our understanding, a strong effort on the event generators is needed.

Channels which don't depend strongly on the Monte Carlo models as polarization measurements at HERA, double tag events or resonance formation at LEP provide clean and unambiguous tests of theoretical ideas.

I express my wish that this field of research, which is sometimes considered marginal, will further develop as a reliable testing ground for QCD calculations.

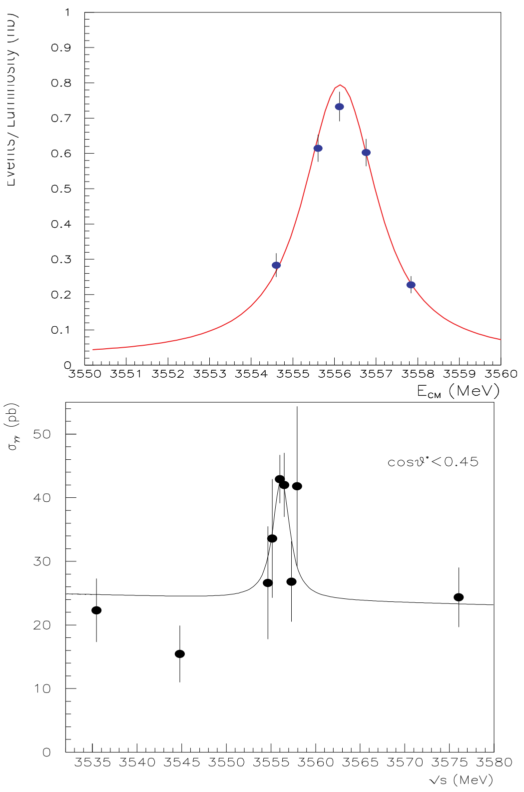

Figure 20. *The E835 χ_{c2} measurement [51]: (top) The event rate for the reaction $p\bar{p}$ $\rightarrow$J/$\psi\gamma$. (bottom) The cross section for $p\bar{p} \rightarrow \gamma\gamma$.*

ACKNOWLEDGEMENTS

I will like to thank Stefan Söldner-Rembold for the lively atmosphere of the Conference and for the perfect organisation. I express my gratitude to Maneesh Wadhwa who helped me in the compilation of LEP data and to Richard Nisius who

provided the QED structure function compilation. Needless to say that this summary is the fruit of all the analysis work pursued at HERA and LEP.

REFERENCES

1. R. Nisius, These proceedings.
2. C. Glasman, These proceedings.
3. R. Engel, These proceedings.
4. M. Pennington, These proceedings.
5. L3 Coll., M. Acciarri et al., Phys. Lett.B 436 (1998) 403; Phys. Lett.B 447 (1999) 147; and F. Erne, These proceedings.
6. ALEPH Coll.,R. Barate et al., CERN-EP/99-0.63 (1999) and A. Böhrer, These proceedings.
7. DELPHI Coll., Igor Tyapkin in "Workshop on Photon Interactions and the Photon Structure" LUND (1998)
8. OPAL Coll., E. Clay, These proceedings.
9. A. Finch, These proceedings.
10. G. Marchesini et al., Comput. Phys. Commun.67 (1992) 465.
11. R. Engel, Z. Phys.C 66 (1995) 203; R. Engel and J. Ranft, Phys. Rev.D 54 (1996) 4244.
12. T. Sjöstrand, Comp. Phys. Comm. 82 (1994) 74
13. OPAL Coll., K. Ackerstaff et al., Z. Phys.C 74 (1997) 33; Phys. Lett.B 411 (1997) 387; Phys. Lett.B 412 (1997) 225.
14. R. Taylor, These proceedings.
15. G.A. Schuler and T. Sjöstrand, Z. Phys.C 68 (1995) 607; Phys. Lett.B 376 (1996) 193
16. M. Glück, E. Reya and A. Vogt, Phys. Rev.D 45 (1992) 3986; Phys. Rev.D 46 (1992) 1973
17. DELPHI Coll., A. Zintchenko, These proceedings
    L3 Coll., M. Acciarri et al., Phys. Lett.B 438 (1998) 363
    OPAL Coll., G. Abbiendi et al., CERN-EP/99-010, Submitted to Eur. Phys. J
18. S. Wölfe, These proceedings.
19. B. Andrieu, These proceedings.
20. Y. Yamazaki, These proceedings.
21. Sung Won Lee, These proceedings.
22. B. Naroska, These proceedings.
23. K. Daum, These proceedings.
24. O. Deppe, These proceedings.
25. N. Gogitidze, These proceedings.
26. A. Valkarova, These proceedings.
27. B. Surrow, These proceedings.
28. Zeus Coll., M. Derrick et al. Phys. Lett.B 384 (1996) 401
29. Physics at LEP2; CERN96-01
30. L3 Coll., M. Acciarri et al., Phys. Lett.B 408 (1997) 450
    and A. Csilling, These proceedings.
31. F. Wäckerle, These proceedings.
32. H.G. Dosch, These proceedings.
33. A. Corsetti, R.M.Godbole and G.Pancheri, Phys. Lett.B435 (1998) 441.
    and G. Pancheri, These proceedings.
34. G.A. Schuler and T. Sjöstrand, Nucl. Phys.B 407 (1993) 539 ; and Z. Phys. C 73 (1997) 677.
35. M. Przybycien, These proceedings.
36. P. Achard, These proceedings.
37. J. Bartels, A. De Roeck, C. Ewerz and H. Lotter, Phys. Lett.B 389 (1996) 742;
    S.J. Brodsky, F. Hautmann and D.E. Soper, Phys. Rev.D 56 (1997) 6957
38. M. Boonekamp, A. De Roeck, C. Royon and S. Wallon, hep-ph/9812523;
    S.J. Brodsky, V.S. Fadin, V.T. Kim, L.N. Lipatov and G.B. Pivovarov, hep-ph/99101229
39. R. McNeil, These proceedings.
40. J. Patt, These proceedings.
41. A. Solano, These proceedings.
42. P. Thomson, These proceedings.
43. R. Wichmann, These proceedings.
44. B. Waugh, These proceedings.
45. D. Ryckbosh, These proceedings.
46. J. Paar, These proceedings.
47. S. Saremi, These proceedings.
48. BES Coll., J.Z. Bai et al. Phys. Rev. Lett.76 (1996) 3502;
    Mark III Coll. R.M. Baltrusaitis Phys. Rev. Lett. et al.56 (1986) 107
49. I. Vodopianov, These proceedings.
50. A. Buijs, These proceedings.
51. M. Stancari, These proceedings.
52. T. Feldmann and P. Kroll, Phys. Lett.B 413 (1997) 410
53. TPC/2γ Collab., D.A. Bauer et al., Phys. Lett. B 302 (1993) 345;
    CLEO Coll., J. Dominick et al., Phys. Rev.

D 50 (1994) 4265;
OPAL Coll., K. Ackerstaff et al., Phys. Lett. B 439 (1998) 197;
L3 Coll.,M. Acciari et al., Phys. Lett. B 453 (1999) 73.

54. E760 Coll., T.A. Armstrong et al., Phys. Rev. Lett.70 (1993) 2988.
55. DELPHI Coll., P. Abreu et al., Phys. Lett.B 441 (1998) 479.